Development 124, 2451-2461 (1997)
Printed in Great Britain © The Company of Biologists Limited 1997
DEV1155

Involvement of programmed cell death in morphogenesis of the vertebrate inner ear

Donna M. Fekete*, Sheila A. Homburger, Michael T. Waring, Ann E. Riedl and Luis F. Garcia

Department of Biology, Boston College, 140 Commonwealth Avenue, Chestnut Hill, MA 02167, USA

*Author for correspondence at present address: Department of Biological Sciences, Purdue University, West Lafayette, In 47907, USA (e-mail: dfekete@bilbo.bio.purdue.edu)

SUMMARY

An outstanding challenge in developmental biology is to reveal the mechanisms underlying the morphogenesis of complex organs. A striking example is the developing inner ear of the vertebrate, which acquires a precise three-dimensional arrangement of its constituent epithelial cells to form three semicircular canals, a central vestibule and a coiled cochlea (in mammals). In generating a semicircular canal, epithelial cells seem to 'disappear' from the center of each canal. This phenomenon has been variously explained as (i) transdifferentiation of epithelium into mesenchyme, (ii) absorption of cells into the expanding canal or (iii) programmed cell death. In this study, an in situ DNA-end labeling technique (the TUNEL protocol) was used to map regions of cell death during inner ear morphogenesis in the chicken embryo from embryonic days 3.5-10. Regions of cell death previously identified in vertebrate ears have been confirmed, including the ventromedial otic vesicle, the base of the endolymphatic duct and the fusion plates of the semicircular canals. New regions of cell death are also described in and around the sensory organs. Reducing normal death using retrovirus-mediated overexpression of human *bcl-2* causes abnormalities in ear morphogenesis: hollowing of the center of each canal is either delayed or fails entirely. These data provide new evidence to explain the role of cell death in morphogenesis of the semicircular canals.

Key words: vertebrate, chick, semicircular canal, apoptosis, otocyst, retrovirus, epithelial fusion, TUNEL, *bcl-2*

INTRODUCTION

The vertebrate inner ear arises from an epithelial thickening on the surface of the head that invaginates and pinches off to form an independent fluid-filled vesicle, called the otocyst (Alvarez and Navascués, 1990; Fritzsch et al., 1997). From this simple vesicle there is a gradual emergence and enlargement of the component parts of the inner ear. In higher vertebrates, each of the three semicircular canals arises from a flattened pouch of epithelium that evaginates from the otocyst (Fig. 1A). The apposing walls of the pouch approach and contact each other over an extensive region called the 'fusion plate' (Fig. 1B). In lower vertebrates, the apposing surfaces direct thinner, finger-like projections (called axial protrusions) into the lumen of the otocyst; these also meet to form a fusion plate (Waterman and Bell, 1984; Haddon and Lewis, 1996). The driving force propelling the walls inward may be generated by secretion of hyaluronan into the subepithelial space (Haddon and Lewis, 1991). After meeting at the fusion plate, the epithelial cells intercalate by an unknown mechanism to form a single layer, at least in the mouse (Martin and Swanson, 1993). At the zebrafish fusion plate, processes of cells from apposing surfaces interdigitate, the basal surfaces of the cells become irregular, and eventually the cells round up and separate (Waterman and Bell, 1984). The disruption of the epithelial sheet leaves a 'hole' where the fusion plate had been (Fig. 1C, asterisks); the remaining structure is now properly called a semicircular canal.

The fate of the cells that 'disappear' from the fusion plate is still under debate. Different models propose that these cells either die, transdifferentiate into mesenchymal cells and migrate away, or become recruited back into the canal epithelium (see discussion by Martin and Swanson, 1993). A similar debate exists with respect to palate formation, where bilateral epithelial sheets of the palatal shelves approach each other, fuse into a 'midline seam' and then disappear to form the roof of the mouth (see discussion by Schuler et al., 1992).

In the case of the fusion plates of the semicircular canals, one can ask whether evidence exists to support a role of programmed cell death. The presence of dying epithelial cells at the fusion plate locale has not been seen consistently in all vertebrate ears: it was not mentioned in comprehensive histological analyses of chicken (Knowlton, 1967), mouse (Martin and Swanson, 1993) or zebrafish (Waterman and Bell, 1984), although it was seen in *Xenopus* (Haddon and Lewis, 1991). The technical advance of using the TUNEL protocol to detect apoptotic cells during normal development has not previously been applied to study the vertebrate inner ear. We have used this approach to confirm the existence of several regions of cell death in the developing chicken ear, including the fusion plates. Furthermore, we report that semicircular canal fusion can be blocked using retrovirus-mediated gene transfer of the human *bcl-2* gene to inhibit normal programmed cell death. These data demonstrate a requirement for cell death in patterning a complex epithelial structure in addition to its known role in patterning mesenchyme of the vertebrate limb bud (Hammar and Mottet, 1971).

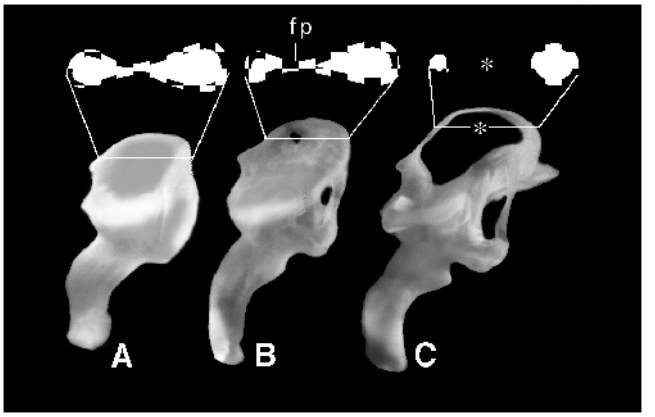

Fig. 1. Semicircular canal formation. Below, the fluid cavities of three different left ears from E6 (A,B) and E6.5 (C) are viewed by the paint-fill method (Bissonnette and Fekete, 1996). Above each is a schematic cross-section through the superior canal, with the lumen in white and the epithelial layer in gray. The two sides of the canal pouch meet at the fusion plate (fp), which ultimately clears (asterisk), leaving the toroidal-shaped canal. Anterior is to the left, dorsal is up.

MATERIALS AND METHODS

Chick embryos

Fertilized, specific-pathogen-free White Leghorn chick eggs were obtained from SPAFAS, Inc. (Norwich, Connecticut). Eggs were incubated at 37.5°C. The first 24 hours of incubation were considered embryonic day 0 (E0). Embryos were also staged according to Hamburger and Hamilton (1951).

Retroviral infections

To obtain high-titer viral stocks, pRCASBP(B) or pRCASBP(B)/*bcl-2* DNA (Givol et al., 1994) was transfected into line 0 chicken embryo fibroblasts (CEFs), cells were expanded for 7-10 days, culture supernatant was collected, concentrated by centrifugation and titered on line 0 CEFs as described (Morgan and Fekete, 1996). Titers of 2-8×10^8 infectious units/ml were used to inject embryos. For injections performed prior to stage 14, viral inoculum was directed to the surface epithelium by (1) injecting above the epithelial surface near the anterior neuropore and also adjacent to each otic placode or (2) delivering excess virus to the neural tube, causing the inoculum to pour out the anterior neuropore and bathe the surface of the embryo (Homburger and Fekete, 1996). Another series of embryos received injections of virus directly into the otic vesicle at stages 16-21. The latter protocol restricts infection to tissues in the immediate vicinity of the inner ear while the former protocol yields widespread infection of embryos (Fekete and Cepko, 1993; Kiernan and Fekete, 1997). Animal care was in accordance with institutional guidelines.

Paint filling of the inner ear

Embryos were decapitated and the heads were fixed, dehydrated, and cleared (Martin and Swanson, 1993). An opaque paint suspension was delivered to the inner ear, which was then photographed and digitized using Adobe Photoshop as described (Bissonnette and Fekete, 1996). Injected ears were compared to a standard atlas of the inner ear prepared by the same method (Bissonnette and Fekete, 1996).

TUNEL protocol

In some cases, ApopTag Peroxidase Kits (Oncor) were used according the manufacturer's recommendations. In other cases, the TUNEL protocol (Gavrieli et al., 1992) was modified as follows: frozen or paraffin-processed sections were postfixed with 4% paraformaldehyde and 0.2% glutaraldehye in PBS, treated with 1 μg/ml of Proteinase K for 4 minutes, washed, immersed in 3% H_2O_2 in methanol for 10 minutes, washed, incubated in TdT buffer (140 mM sodium cacodylate, 1 mM $CoCl_2$ in 30 mM Tris, pH 7.2) for 2 minutes, incubated in terminal transferase reaction mix (0.17 u/ml of TdT [USB, Amersham], 1.25 nM biotin-14-dCTP; 0.1% BSA in TdT buffer) for 60 minutes at 37°C, incubated in TB buffer (30 mM sodium citrate, 300 mM NaCl) for 15 minutes, washed in water twice for 5 minutes, processed with ExtrAvidin Peroxidase (diluted 1:100 in 0.1% BSA) as described in Gavrieli et al. (1992), and reacted with diaminobenzidine (0.5 mg/ml, 0.01% H_2O_2 in 0.25 M Tris buffer, pH 7.2) for 3-4 minutes.

Accurate quantification of the number of dying cells was difficult for several reasons. First, there is the tendency for cells to break apart, leading to more than one TUNEL-positive profile for each cell. Second, at the beginning and end of apoptosis, a dying cell may only be detectable as a small TUNEL-positive fragment that is much less than the average diameter of the nucleus. Third, cell debris is cleared by macrophages, leading to clumping of numerous apoptotic profiles within a single macrophage. In quantifying the degree of apoptosis, we scored separately each TUNEL-positive profile that had a distinct external border and a diameter greater than approximately one-fourth of a cell nucleus, regardless of the degree of clumping; there were many examples of such profiles occurring in isolation. Counts were made from every third section through the fusion plate region including, after clearing, positive profiles located within the canal proper or among the mesenchyme.

Immunohistochemistry

Indirect immunohistochemistry using the Vectastain ABC-HRP kit (Vector Laboratories) has been described (Fekete and Cepko, 1993), except that primary antibodies were incubated overnight at 4°C. For embryos injected with RCASBP(B)/*bcl-2*, the primary antibody was a mouse monoclonal anti-bcl-2 directed against human protein (but not mouse or chicken) from Oncogene Science, used at 1:300 dilution. For embryos injected with RCASBP(B) parent virus, the primary antibody was culture supernatant from 3C2 mouse hybridoma cells making antibody against viral $p19^{gag}$ matrix protein; supernatant was used at 1:1 dilution.

Detection of the basal lamina was done using indirect immunofluorescence with a mouse monoclonal IgM directed against a highly conserved epitope (10E4) of human heparan sulfate (Seikagaku Corporation, Tokyo, Japan). Simultaneously, sections were incubated with a mouse monoclonal IgG antibody, HCA, directed against a hair cell antigen, which detects the apical surfaces of hair cells (Bartolami et al., 1991). The protocol was as follows: fixed, frozen sections were thawed, postfixed for 10 minutes in 4% paraformaldehyde in PBS, washed and incubated in blocking solution (3% bovine serum albumin, 1% horse serum, 0.05% Triton X-100 in PBS). All incubations were performed at room temperature. Tissue was incubated in primary antibodies (anti-heparan sulfate antibody at 1:250 and anti-HCA at 1:500 in blocking serum without detergent) for 1 hour. After washing in PBS, tissue was incubated in biotin anti-mouse IgM (Vector, 1:200) and biotin anti-mouse IgG (Vector, 1:250) diluted in blocking serum for 1 hour, washed in PBS and incubated in CY2-Streptavidin (Biological Detection System, 1:250) in blocking serum without detergent for 1 hour. After washing in PBS, tissue was coverslipped using carbonate-buffered glycerol with paraphenylenediamine (1 mg/ml) to reduce photobleaching and viewed with a Zeiss Axioplan.

RESULTS

Programmed cell death during inner ear development

To ascertain whether programmed cell death occurs during

normal development of the chicken ear, we using variations of the TUNEL protocol to label fragmented ends of DNA in situ on fixed paraffin sections (Gavrieli et al., 1992). Labeled cells were evident in all specimens studied from E3.5 to E7; labeled cells were either scattered or grouped together in patches. From E8-E10, labeled cells were seen only rarely. Within the time window of E3.5-E7, certain regions consistently showed large numbers of labeled cells, ranging from tens to hundreds of TUNEL-positive profiles. Some of these regions, which we refer to as 'hot spots', were seen at places throughout early ear morphogenesis where the otic epithelium was making obvious constrictions or bends. Others were correlated with particular morphogenetic events and will be discussed in turn.

The otic vesicle pinches off from the overlying ectoderm on E2. Around this time, cells begin to delaminate from the vesicle and migrate medially to form the sensory ganglion of the eighth cranial nerve (VIIIg). In addition, during the next several days, the endolymphatic duct elongates dorsomedially, while the anlagen of the cochleosaccular duct protrudes ventrally. All three of these morphogenetic events are accompanied by localized hot spots of cell death.

The first hot spot of cell death was located adjacent to the VIIIg in the ventral wall of the otic vesicle. At E3.75, a cluster of these cells appeared to coincide with the location of the source of emigrating VIIIg cells on the ventrolateral edge (Fig. 2A,B, arrows). This restricted hot spot was one of the smallest identified. A few labeled cells were also observed immediately beneath the otic epithelium at this location (Fig. 2B, arrowhead) and within the stream of migrating VIIIg cells (data not shown).

The most impressive and prolonged hot spot of cell death was observed on the ventromedial wall of the otocyst. At E3.75, the degree of cell death in this region was variable both within and across individuals: of four ears studied, two contained dozens of labeled cells, while two did not. By E4.5, the ventromedial hot spot was consistently observed near the proximal part of the elongating ventral (cochleosaccular) duct. This region continued to display hundreds of TUNEL-positive profiles throughout the period from E5 to E7. Examples of this hot spot are shown at E5.25 (Fig. 2C,D, vm), E5.8 (Fig. 2E, arrowhead) and E6.8 (Fig. 2G, arrowhead). As soon as the cochlear duct began to elongate, the hot spot appeared to wrap around the neck of the duct anteriorly, forming a hemi-collar of labeled cells (Fig. 2E,G). Beyond E7, the ventromedial hot spot was not observed.

Like the cochlear duct, the endolymphatic duct also had an associated cluster of labeled cells near its origin in the otic vesicle (Fig. 2C,D, arrow). Although not yet evident on E3.5 (a time when the duct was quite obvious), a hot spot of cell death was seen in this location over the next several days.

The lateral wall of the cochlear duct had labeled cells scattered throughout its length on E5-7, with a greater preponderance of labeled cells observed proximally (Fig. 2G, arrow).

As the sensory organs began to differentiate, additional hot spots of cell death appeared. After identifying hot spots of cell death with the TUNEL protocol, their relationship to developing sensory organs was assessed by labeling adjacent sections with a monoclonal antibody (anti-HCA) directed against a hair cell antigen (Bartolami et al., 1991). TUNEL-labeled cells were observed within and/or near the saccular macula, the utricular macula, the cristae of each semicircular canal and the basilar papilla at E6-7 (Fig. 3). In some cases, the TUNEL-labeled cells appeared to be coextensive with a region of differentiating hair cells, typically located beneath the hair cells

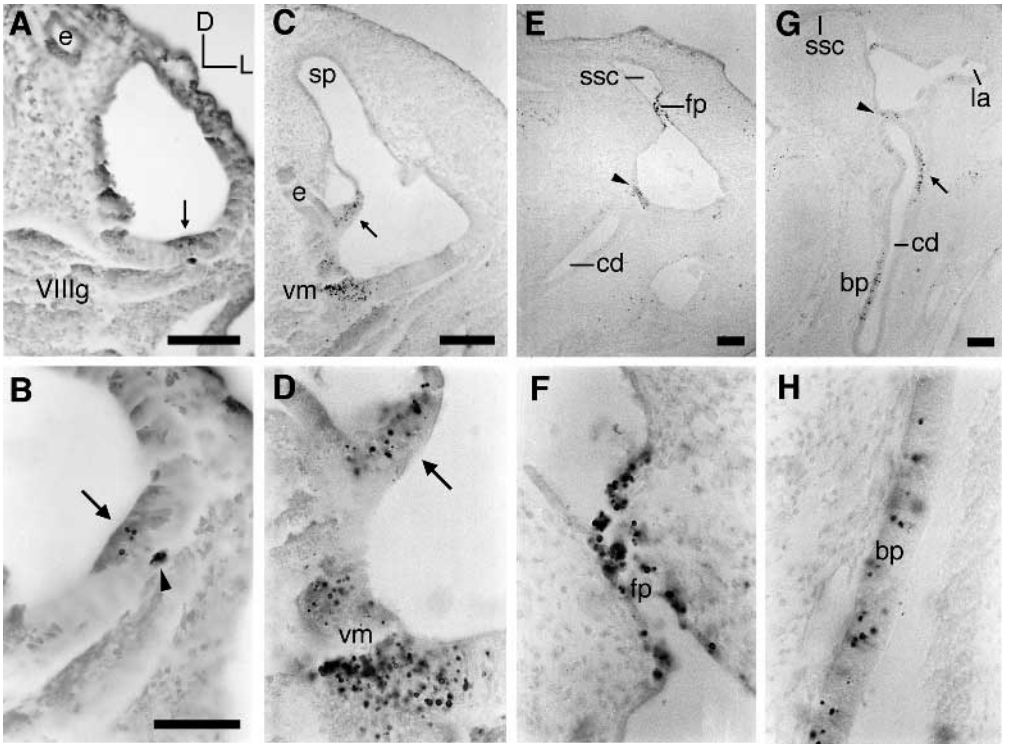

Fig. 2. Hot spots of cell death during inner ear development detected by the TUNEL protocol. (A,B) E3.75 (stage 23) ear, showing labeled cells (arrow) adjacent to cells of the eighth cranial ganglion (VIIIg). A small cluster of apoptotic profiles can be seen beneath the epithelium (arrowhead). Orientation of dorsal (D) and lateral (L) is shown. (C,D) E5.25 (stage 26) ear, showing labeled cells in the ventromedial hot spot (vm) and adjacent to the endolymphatic duct (arrow). The superior pouch (sp) which will give rise to the superior semicircular canal has few labeled cells. (E,F) E5.8 (stage 28) ear showing the ventromedial hot spot of cell death (arrowhead) near the neck of the cochlear duct (cd), and at the fusion plate (fp) of the superior semicircular canal (ssc). (G,H) E6.8 (stage 29) showing several hot spots of cell death, including the neck of the cochlear duct (arrowhead), the lateral wall of the duct proximally (arrow), the medial wall of the duct distally, where the basilar papilla (bp) is forming, and near the lateral ampulla (la). Scale bars for the top row are 100 μm; scale bar in B is for the bottom row and is 50 μm.

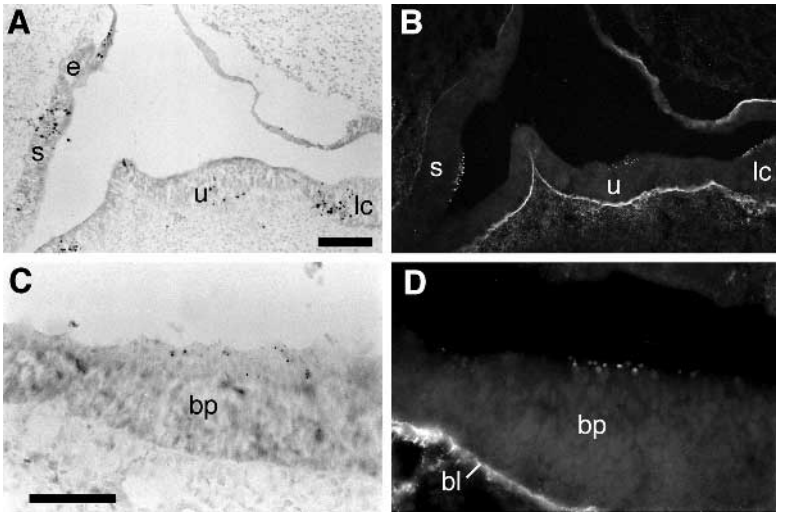

Fig. 3. Cell death in and near forming sensory organs. (A,C) Cell death is detected using the TUNEL protocol. (B,D) Indirect immunofluorescence is used to detect the apical surfaces of differentiating hair cells (small punctate spots near the lumen of the ear) using HCA antibody and the basal lamina (bl) of the inner epithelium using antibody against heparan sulfate. (A,B) E6.75 ear (stage 28.5). Regions of cell death lie in or adjacent to the saccular macula (s), the utricle (u), the lateral crista (lc) and the endolymphatic duct (e). (C,D) E6.75 (stage 28) basilar papilla (bp) with only a few hair cells just beginning to express HCA; this region shows faint evidence of dying cells, both apically in the epithelium (among hair cell nuclei) as well as further basally (among supporting cell nuclei). Scale bar in A is 100 μm and in C is 50 μm.

on the basal half of the sensory organ; the utricular macula is shown as an example (Fig. 3A,B). In other cases, TUNEL-positive profiles were found apically in the sensory epithelium (such as in the basilar papilla of Fig. 3C,D). Finally, dozens of TUNEL-labeled profiles were found immediately adjacent to HCA-immunoreactive regions (such as the saccular macula and crista of Fig. 3A,B). In the basilar papilla, a localized patch of cell death was observed distally, before the hair cell antigen could be detected (Fig. 2G,H). By the time the first HCA-positive region was detected in the distal basilar papilla (late on E6), a few TUNEL-positive profiles appeared to overlap spatially with the hair cells (Fig. 3C,D), as evidenced by examination of adjacent sections. In this case, the minute size of the TUNEL-positive profiles (compare Fig. 3C to Fig. 2H taken at the same magnification) suggests that they may represent a late stage of apoptosis. In general, however, it was difficult to detect overlap between the HCA-positive region and the TUNEL-positive region on the basilar papilla; instead, most of the cell death was located adjacent to patches of differentiating hair cells (data not shown).

Finally, a massive hot spot of cell death was associated with the fusion plate of each of the semicircular canals. Because these regions were especially vulnerable to perturbation of cell death, as detailed later, they will be discussed separately in the next section.

Cell death during semicircular canal fusion

Fusion of the semicircular canals occurs very quickly at the beginning of the 6th day of incubation (Bissonnette and Fekete, 1996), and so this period was studied in detail. The results consistently showed extensive cell death at the fusion plates of all three semicircular canals (Figs 2E,F, 4). The timing of the cell death was found to correlate closely with the apposition of the two epithelial sheets. Cell death was first observed in the center of each canal pouch at the time of initial contact between apposing epithelial surfaces. It then appeared to spread radially to include adjacent cells that were not yet making contact on their apical surfaces with cells of the apposing sheet (Figs 2F, 4D). In some specimens, one of the two epithelial sheets had many more labeled cells than the other; however, there was tremendous variability in this respect and cell death did not seem to be consistently restricted to one side of the fusion plate. Instead, many examples were seen in which cell death was nearly symmetric in the two apposing surfaces from the earliest stages in which it was seen. As the fusion plates enlarged and thinned, dying cells were observed throughout the entire area (Fig. 4B).

Among the three canals, the order in which cell death first appeared mirrors the order of their development. That is, the superior and posterior pouches fuse in advance of the lateral, and likewise individual specimens were found in which the fusion plates of the former two pouches contained numerous labeled cells, while the lateral pouch had none (Fig. 4A-D). Specimens that were slightly more advanced had numerous labeled cells in all three fusion plates (data not shown). At all stages, the posterior canal fusion plate was the smallest of the three canals.

As canal fusion commenced during the sixth embryonic day, the labeled cells accumulated along the entire inner circumference of the enlarging canals (Fig. 4H, arrows). Other labeled cells could be found scattered among the mesenchymal cells that were encroaching into the space where the fusion plate had been (Fig. 4F-G, arrowheads). On E6.75, cell counts of every third section revealed that hundreds of labeled cells were still present in and near each canal (Table 1). By E7, the canals were always cleared (Fig. 4F-H, asterisks), except for the lateral canal in rare cases where the embryos looked generally unhealthy. At E7, many TUNEL-positive cells were still evident. By E8 and E9, labeled cells were extremely rare in or near the semicircular canals (data not shown).

Inhibition of semicircular canal formation by infection with a *bcl-2*-expressing retrovirus

One way to assess the role of apoptosis during normal ear development is to interfere with the process and see whether or not phenotypic defects are generated (Hay et al., 1994). The human *bcl-2* gene was used for this purpose, since it has been shown to block a final common pathway for programmed cell death under a variety of experimental conditions, both physiological and pathological (reviewed by Reed, 1994; Davies, 1995). RCASBP(B)/*bcl-2* is a replication-competent avian retroviral vector encoding human *bcl-2*; this virus was shown to be physiologically active in vitro when introduced into chicken embryo fibroblasts (Givol et al., 1994). Such a virus

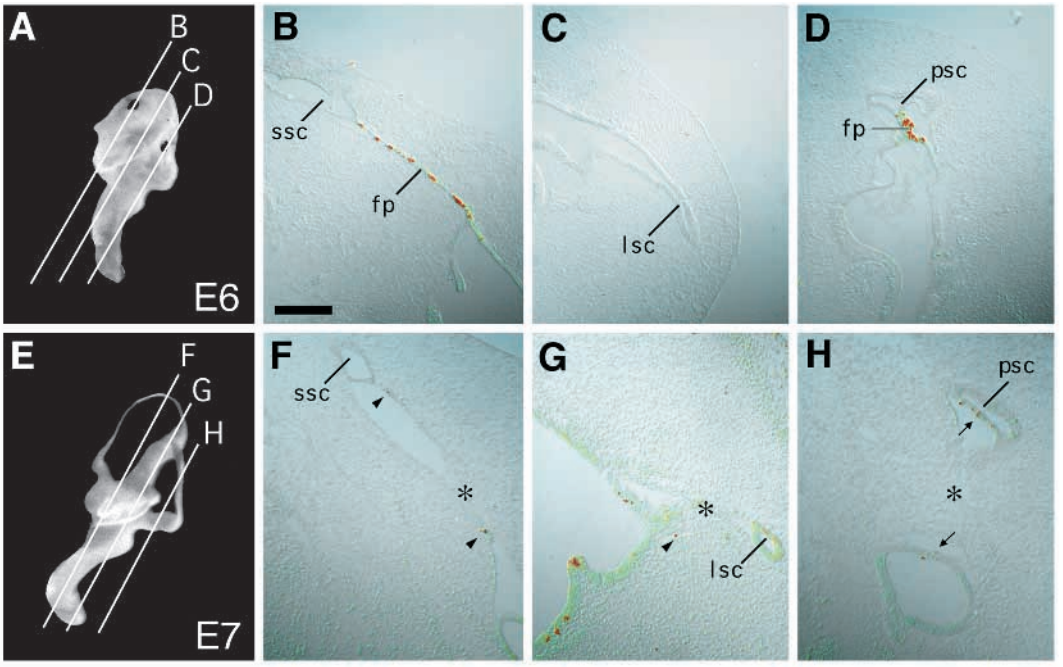

Fig. 4. Cell death and semicircular canal formation. (A,E) Paint-filled inner ears illustrate the approximate planes of section through the superior (ssc), lateral (lsc) and posterior (psc) semicircular canals for specimens at E6 (B-D) and E7 (F-H). Sections were stained with variations of the TUNEL protocol to detect apoptotic cells. On E6, fusion plates (fp) contained numerous apoptotic cells. By E7, the fusion plates of all three canals were cleared (asterisks), leaving behind scattered dying cells in their place (arrowheads) or along the margins of the enlarging canals (arrows). In the sections, dorsal is up, medial is to the left, and scale bar in A is 100 μm.

can infect and spread through a target population of cells in vivo, greatly increasing the number of 'transgenic' cells (Morgan and Fekete, 1996; Kiernan and Fekete, 1997). High titer viral stocks were injected into E1.5-3.5 chicken embryos at stages ranging from 8-22. Control virus injections were done using the parent vector, RCASBP(B), at similar titers.

Embryos were processed at ages ranging from E6.5-11 (stages 28-37). To evaluate the ear for changes in three-dimensional morphology, specimens were cleared and the fluid cavities of the ear were filled with an opaque paint suspension. Specimens were then embedded in paraffin and sectioned, allowing canal morphology to be further studied at the histological level. Inner ear morphology was assessed in 104 ears (from 63 embryos) that received *bcl-2*-encoding retrovirus, in 37 infected control ears (from 21 embryos) that received the parent virus, and in numerous uninjected control ears. Uninjected control ears (Fig. 5A) and injected control ears (data not shown) were indistinguishable by the paint-fill assay. Gross morphological defects resulting from *bcl-2* overexpression were limited to the semicircular canals, with the caveat that, in many ears, the morphology of the ventral cochlear duct housing the basilar papilla was obscured due to spillage of paint into the mesenchyme surrounding the ventral part of the ear.

Of the bcl-2-infected ears, 39% (41 of 104) showed a clear defect in canal fusion, never progressing beyond the pouch stage as judged by paint filling. The defect was restricted to the posterior canal in all but one ear, which had a defective lateral canal (Fig. 5B-D). This phenotype was observed with greater frequency following injections performed at earlier stages: 55% for stages 6.5-9 (28 of 51); 33% for stages 9.5-12 (13 of 39) and 0% for stages 13-21 (0 of 14). Unfused posterior pouches were observed as late as E10.5 in bcl-2-infected ears, while this was never observed for any of the canals at E6.5 or beyond in infected control embryos.

Examination of serial sections through 66 ears revealed a more subtle phenotype in all three canals: fusion plate clearing was delayed by up to 36 hours. Abnormally long appositions of the two sides of the canal generated elongated fusion plates. When no area of clearing was apparent in these abnormal

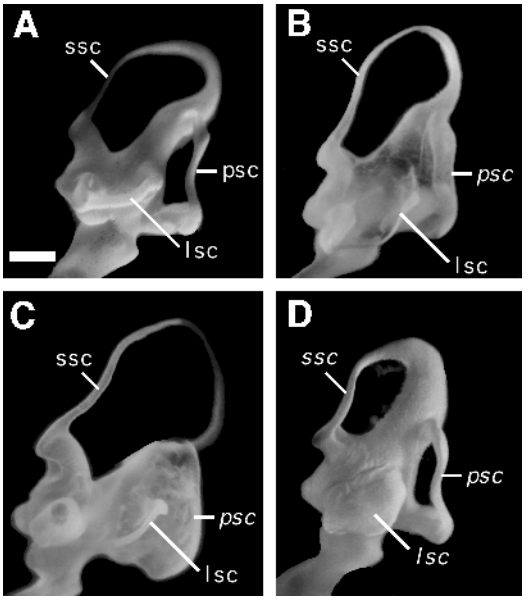

Fig. 5. Phenotypic defects in semicircular canal formation following overexpression of *bcl-2*. (A) E6.5 uninjected control embryo from the same batch as those shown in B-D. Filling the lumen of the ear with paint indicated that all three canals were well-formed. (B-D) Defective canals (italics) were evident following injection of RCASBP(B)/*bcl-2* on E1.5. The posterior canal was affected most frequently, shown here at E6.5 (B) or E8.5 (C). In one case (D) the lateral canal was defective at E6.5; this ear also showed evidence of a delay in development of the superior canal. Abbreviations: lsc, lateral semicircular canal; psc, posterior semicircular canal; ssc, superior semicircular canal. Italics are used to indicate phenotypically abnormal structures. Scale bar is 500 μm.

Table 1. The effect of *bcl-2* misexpression on development and cell death in the semicircular canals

		SSC			LSC			PSC		
Ear	Age	Phenotype	No. TUNEL+ profiles	Degree of infection	Phenotype	No. TUNEL+ profiles	Degree of infection	Phenotype	No. TUNEL+ profiles	Degree of infection
RCASBP(B)/bcl-2 - INJECTED										
H38.6R#	E7	2	29	***	2	49	***	2	26	***
H38.6L#	E7	2	26	***	2	33	***	2	77	***
H38.33R	E6.75	1	75	***	2	20	***	2	6	***
H38.33L	E6.75	0	116	***	2	87	***	2	37	***
H39.2R	E6.75	1	18	*	1	147	*	2	58	*
H39.2L	E6.75	0	n.d.	***	0	n.d.	***	2	33	***
H39.3R	E6.75	2	132	***	2	88	***	2	42	***
H39.3L	E6.75	1	172	***	2	98	***	2	66	***
H39.5R	E6.75	0	243	*	2	95	**	1	27	***
H39.5L	E6.75	1	40	***	2	23	***	2	44	***
H39.6R	E6.75	2	260	***	2	52	***	2	53	***
H39.6L	E6.75	2	172	***	2	71	***	2	60	***
Mean Number			**117**			**69**			**44**	
S.D.			**87**			**38**			**20**	
% of injected controls			**0.33**			**0.18**			**0.13**	
RCASBP(B) - INJECTED CONTROLS										
H38.16R#	E7	0	n.d.	***	n.d.	n.d.	***	0	398	***
H38.16L#	E7	0	435	***	2	286	***	0	336	***
H38.43R	E6.75	0	263	***	1	n.d.	***	0	n.d.	***
H38.43L	E6.75	0	324	***	1	518	***	0	281	***
H39.13R	E6.75	0	380	*	0	663	*	0	453	*
H39.13L	E6.75	0	478	*	0	347	*	0	390	*
H39.15R	E6.75	0	318	***	0	280	***	0	225	***
H39.15L	E6.75	0	265	***	0	269	***	0	293	***
Mean Number			**352**			**394**			**339**	
S.D.			**83**			**161**			**79**	
UNINJECTED CONTROLS										
H38.3R	E7	0	225		0	168		0	134	
H38.3L	E7	0	237		0	634		0	212	
H38.12R	E7	0	218		0	198		0	194	
H38.12L	E7	0	229		0	286		0	189	
H39.8R	E6.75	0	251 +		0	159 +		0	160	
H39.8L	E6.75	0	210		0	270 +		0	192 +	
H39.19R	E6.75	0	526		0	456		0	356	
H39.19L	E6.75	0	n.d.		0	656		0	597	
Mean Number			**271**			**353**			**254**	
S.D.			**113**			**203**			**153**	

Phenotype: (0), normal – large canal opening; (1) abnormal – elongated fusion plate with small opening;
(2) more severe – canals not open, fusion plate present.
Degree of infection is the approximate percentage of infected cells: (*) less than 33%; (**) 33-66*; (***) greater than 66%
(#), animal looked unhealthy at harvest.
(+), at least two sections missing through the canal so additional TUNEL-positive profiles could be present.
(n.d.), not determined due to technical or histological artifacts.

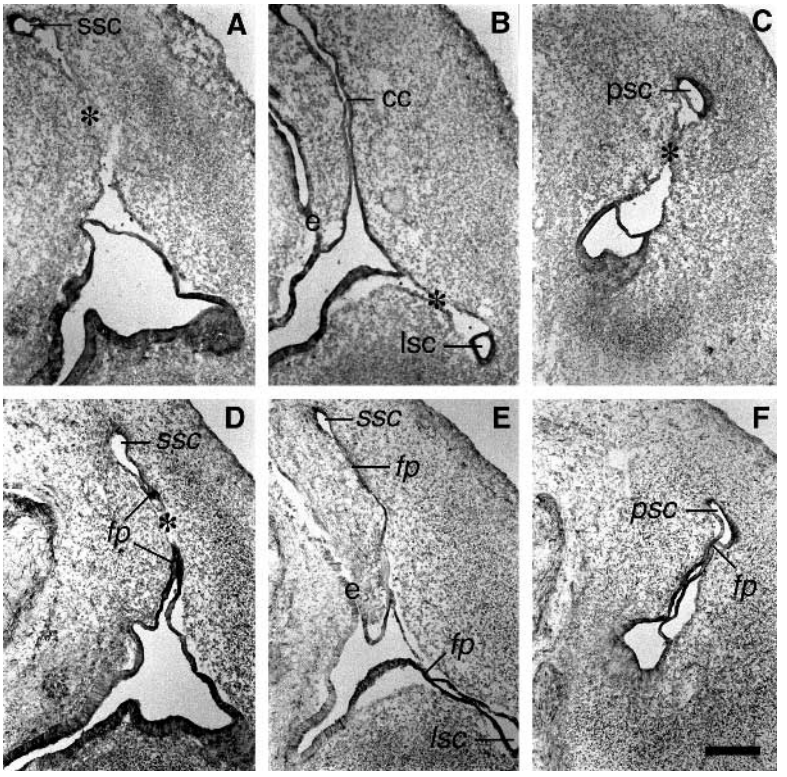

Fig. 6. Semicircular canal formation is disrupted by blocking programmed cell death. (A-C) Sections through a control ear from an E6.75 embryo injected with RCASBP(B) parent virus at stage 12; indirect immunohistochemistry was used to detect viral matrix protein. Canal plate fusion and clearing (asterisks) has occurred normally in all three well-infected canals; in B, the crus communis (cc) connecting the superior and posterior canals is normal (compare to plane G in Fig. 2E). (D-F) Ear from an E6.75 embryo injected with RCASBP(B)/*bcl-2* at stage 9 and processed for immunohistochemistry to detect human bcl-2. The majority of the inner ear epithelium and surrounding mesenchyme were expressing virally encoded proteins. The posterior canal pouch showed no evidence of fusion, while the superior and lateral canals had elongated fusion plates adjacent to small regions which had cleared (asterisk in D; not shown for lateral canal). Scale bar in F is 200 μm. Orientation, abbreviations and symbols as in Fig. 4. e, endolymphatic duct. Italics are used to indicate phenotypically abnormal structures.

fusion plates (Fig. 6F), the phenotype was scored as a '2' (Table 1). Confined regions of clearing were apparent in the center of many of these elongated fusion plates (Fig. 6D), and this phenotype was scored as a '1' (Table 1). In normal ears, such small regions of clearing were observed much earlier, when the overall size of the canals and their fusion plates were proportionally smaller. Elongated fusion plates displaying either phenotype 1 or 2 were observed for two or more canals in 87% of the ears at E6.75-E7 (Fig. 6), 33% at E7.5, 12% at E8.0 and 0% at E8.5. This was unlikely to result from a general delay in ear development, as the overall size of the ear continued to increase at a normal rate (compare Fig. 6A-C to D-F). Eventually, clearing of the fusion plates was completed for all but the posterior canals.

When examined at E6.75, the elongated fusion plates usually comprised two independent epithelial sheets that were apposed for a relatively long distance (Fig. 7D-F). The basal lamina was intact, as evidenced by immunostaining with antibody against heparan sulfate (Fig. 7E). During normal canal fusion, the basal lamina never seems to disappear entirely, but instead remains intimately associated with the canal epithelium; a relatively small and variable amount of basal laminar material remains behind in the central core after canal fusion is complete (Fig. 7A-C).

All three semicircular canals were well infected with virus following injections at stages 8-12

To determine how extensive virus infection was at the critical time of canal plate formation, ears were processed at E6.75 to detect human bcl-2 (n=10) or viral matrix protein (n=6 controls). Others were similarly processed at E7-11.5 to determine the extent of *bcl-2* (n=53) or viral gene expression (n=6 controls) at the time of harvest. For those that had first been paint-filled, tissue was embedded in paraffin, sectioned, dehydrated and immunostained. Otherwise, tissue was fixed in 4% paraformaldehyde, embedded in gelatin, frozen-sectioned and every third section was immunostained. In most cases, either human bcl-2 protein (Fig. 6A-C) or viral matrix protein (Fig. 6D-F) appeared to be widely expressed in all three canals (Table 1), suggesting that the absence of a gross phenotype in canal fusion was unlikely to be the result of any systematic differences in the degree of infection among the three canals at the time of fusion. The few canals that did not appear to be well infected are noted in Table 1.

Infection with a *bcl-2*-expressing virus decreased programmed cell death at the semicircular canal fusion plates

In addition to staining for virally transduced proteins at E6.75-E7, adjacent sections from 26 infected ears were processed using the TUNEL protocol to assess cell death (Fig. 7D,F). Counts were made of TUNEL-positive profiles from every third section through each of the three canals in the vicinity of their central fusion plate regions. For a few of the canals, quantification was not possible due to unacceptably high background staining with the TUNEL protocol, or loss of section integrity during sectioning and staining. Table 1 shows the results of quantifying cell death in experimental and control ears. All 12 ears infected with bcl-2-virus showed significant reduction in the number of apoptotic cells, particularly in the posterior canal and lateral canals, compared with 8 RCASBP(B)-infected control ears and 8 uninjected ears. On average, the posterior canals had only 13% of the number of TUNEL-positive profiles seen in the infected control ears, with a range of 2-23% of control. TUNEL-positive profiles in lateral canals of bcl-2 infected ears were reduced to 18% of control

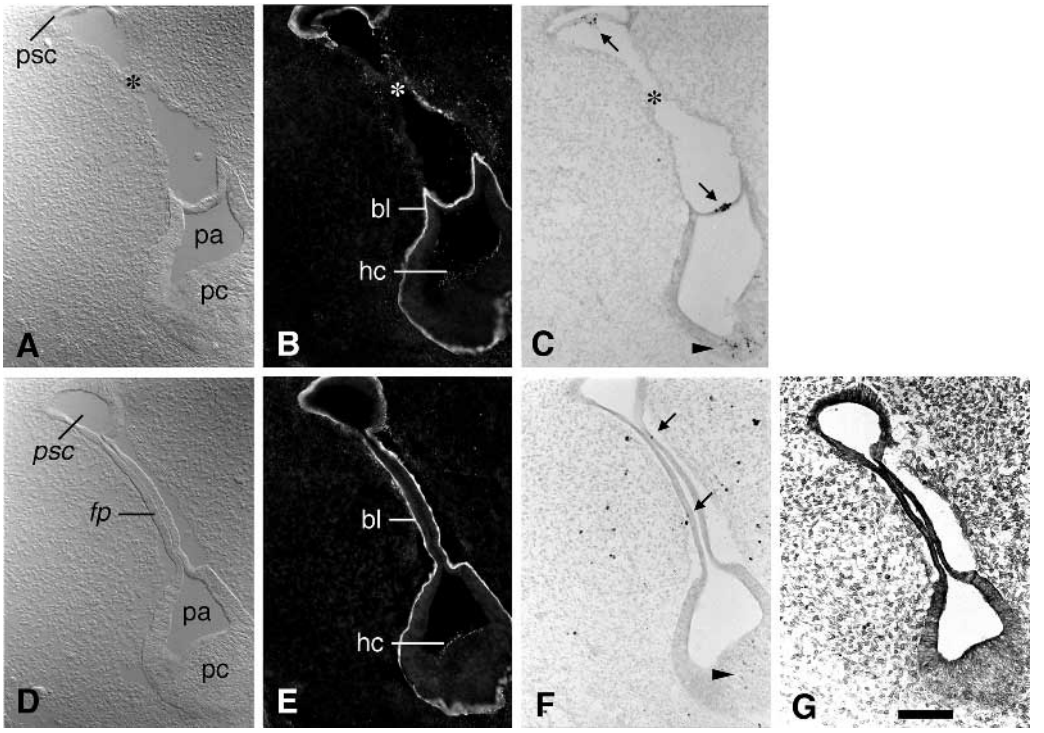

Fig. 7. Semicircular canals with prolonged fusion plates resulting from *bcl-2* misexpression have an intact basal lamina, normal-appearing hair cells and a limited amount of cell death in comparison to control ears. (A-C) Posterior semicircular canal from an uninjected control embryo processed at E6.75. (D-G) Posterior semicircular canal from an E6.75 embryo that was injected with RCASBP(B)/*bcl-2* at stage 12. Control and experimental ears are compared by: (A,D) Nomarski optics; (B,E) immunofluorescent staining with anti-HCA (to detect hair cells) and anti-heparan sulfate (to detect basal lamina); and (C,F) TUNEL-labelling to detect apoptotic cell profiles (arrows) near the fusion plate locale (asterisk) or in the sensory crista (arrowheads). (E) The extent of human bcl-2 protein expression is shown for the injected ear using indirect immunohistochemistry. Abbreviations: bl, basal lamina; fp, fusion plate; hc, hair cell apical staining; pa, ampulla of the posterior semicircular canal; pc, crista of the posterior semicircular canal; psc, posterior semicircular canal. Scale bar in G equals 100 μm. Right canals are shown, with the orientation tilted (compare to Fig. 6) such that dorsal is towards the upper left, and lateral is towards the upper right.

(range 5-37%). The number of TUNEL-positive profiles in the superior canals of bcl-2 infected ears was generally higher and more variable, with an average of 33% of controls and a range of 5-74%. The absolute number of apoptotic profiles in the superior canal epithelium was not strictly correlated with the degree of phenotypic abnormality, showing no evidence of a threshold number below which the canal would be affected (Table 1).

DISCUSSION

Cell death during inner ear development

Programmed cell death was found in many regions of the developing inner ear of the chicken. Some of the regions had been previously described in the chicken, some had been mentioned in other species but not in the chicken and some are reported here for the first time. The earliest stages of otic vesicle formation had already received considerable attention in the literature. In the human embryo, dying cells were observed just prior to and during the stages when the otic pit pinches off from the overlying ectoderm to form the otic vesicle (Represa et al., 1990). At this location, a transient epithelial bridge or stalk connecting the otic vesicle to the ectoderm appeared to contain numerous pyknotic cells; apparently this connection is eliminated by programmed cell death in the human (Represa et al., 1990) and the rat (Marovitz et al., 1977). In a similar location in the stage 15 chicken embryo, cell death appeared to be restricted to the caudal and medial edges of the closing vesicle when viewed by scanning electron microscopy (Alvarez and Navascués, 1990). Although otic vesicle closure was not studied directly here, this phase of cell death was unlikely to have been directly affected by the retrovirus-mediated overexpression of *bcl-2* because of inherent limitations in retrovirus-based gene transfer. Specifically, we have found a minimum delay of 9 hours between the time of infection and the first detectable expression of virally transduced proteins in rare cells of the embryonic neural tube following injections at stages 9-13 (Homburger and Fekete, 1996). Significant protein expression begins to appear about 18-20 hours after infection (stages 15-16) in some animals, with measurable increases in the number of expressing cells continuing out to 48 hours after infection (stages 18-22). With this timetable, the early events of otic vesicle delamination would be finishing about the time that significant protein expression was first expected (around stages 15-18 on E2), while maximal expression would be expected to occur even later (around stages 18-22 on E3).

A second region of cell death was observed among the otic epithelial cells that are located above the developing primordium of the VIIIg along the ventral wall of the otic vesicle. Pyknotic cells were also detected in this region in the human

embryo (Represa et al., 1990). It is unclear whether or not this region develops directly into the larger, more profound region of cell death seen in the ventromedial wall of the otic vesicle at slightly later stages. This ventromedial region was termed the 'otic necrotic zone' by Marovitz et al. (1976, 1977) who observed it in the rat embryo using transmission electron microscopy. In both the rat and the chicken, the ventromedial region of cell death persists for some time during the elongation of the cochlear duct, remaining at the proximal rim of the duct where it meets the saccule. The ventromedial hot spot was evident during stages when virally transduced bcl-2 protein was expected to have decreased cell death. So far, we have seen no evidence of abnormalities in the gross morphology of this region at E6-10 as a result of earlier *bcl-2* misexpression, although shorter harvests would be desirable to ascertain how effectively the gene transfer was reducing cell death in this region.

A hot spot of cell death located near the juncture of the endolymphatic duct with the vestibule of the otic vesicle is described here for the chicken embryo. This same region has been reported for the human embryo (Represa et al., 1990). Again, the timing suggests that *bcl-2* misexpression might be expected to alter cell death in this region, but no phenotypic abnormalities of the endolymphatic duct were evident.

Additional hot spots of cell death were observed in and near developing sensory organs. It is not known what the role of cell death may be in these areas. Perhaps the zones of cell death that occur at the edges of the sensory organs serve to limit the spatial extent of organ formation. Alternatively, they may be involved in the segregation of one sensory anlage from another. The timing of cell death in the basilar papilla suggests that it precedes overt sensory cell differentiation and may be more highly correlated with the commitment of cell fates. This intriguing possibility requires further study, with a focus on the spatial and temporal association between the expression of cell-type-specific markers and the detection of cell death. No obvious defects were evident in the size or location of the sensory organs following *bcl-2* misexpression, although the present study is primarily focused on evaluation of gross morphological phenotypes. An in-depth morphological analysis will be required to fully assess the role of cell death in the formation of sensory epithelia. We have initiated such an analysis using scanning electron microscopy to examine the differentiated sensory epithelium of the basilar papilla following *bcl-2* overexpression; in preliminary studies, we have observed profound perturbations in cellular morphology and patterning of hair cells and supporting cells (Riedl et al., 1997).

In the present study, we have demonstrated the presence of cell death at the fusion plates of the semicircular canals. The interval of cell death in this region is rather brief, with the bulk of it occurring between late E5 and E7. The onset of cell death at the center of the canal pouch generally coincided with contact between apposing epithelial sheets. However, apical contact is unlikely to be the only inductive signal for cell death because, along the outermost rim of the cell death area, dying cells were observed that had not yet made contact with the apposing epithelial cells. It is possible that such cells were signaled laterally, within the plane of the epithelium, by their neighbors, which had made contact on their apical surfaces.

Normal cell death is required for proper canal formation

Retrovirus-mediated gene transfer was used to attempt to block cell death in the developing inner ear by overexpressing the human *bcl-2* gene. This experimental manipulation was successful in delaying, and in many cases preventing, the completion of the fusion process. The block in canal fusion was most apparent for the posterior canal. The selective vulnerability of the posterior canal is puzzling given that the retroviral vector was driving bcl-2 protein expression equally in all three canals, as evidenced by immunostaining for the protein. The posterior canal is neither the first nor the last to initiate fusion, suggesting that the timing of infection relative to the stage of development is not a likely variable to explain posterior canal sensitivity. In contrast, the relative sizes of the fusion plates may be of importance, with the superior canal being largest, the posterior canal smallest and the lateral canal intermediate in size. Perhaps larger canals require a combination of mechanisms to complete clearing, including not only elimination of cells by programmed cell death, but also resorption of some cells into the enlarging outer rim of the canal. The size of the fusion plate might also affect the probability of cells escaping the bcl-2-mediated block. On average, the infected superior canals had the most apoptotic bodies, the lateral canals an intermediate number and the posterior canals the least (Table 1). If the presence of only a few dying cells is adequate to disrupt epithelial cell-cell interactions and initiate fusion, the probability of this occurring (and the canal therefore showing a normal morphology) would be greatest for the superior canal, intermediate for the lateral canal and the least for the posterior canal, as observed.

The fate of fusion plate cells among vertebrates

This study supports the hypothesis that proper morphogenesis of vertebrate semicircular canals requires programmed cell death. The question arises as to how universal this process may be. Among lower vertebrates, canal fusion is accompanied by pyknotic cells and debris indicative of dying cells in *Xenopus* (Haddon and Lewis, 1991), but not in zebrafish (Waterman and Bell, 1984). In the mouse, both light and electron microscopic observation of the fusion plate has failed to indicate the presence of dying cells (Martin and Swanson, 1993). The fate of the fusion plate cells was further studied in the mouse by injecting dye into the lumen of the otocyst, where it was taken up by the canal epithelial cells (Martin and Swanson, 1993). After canal fusion, there were no labeled cells in the mesenchyme, refuting the hypothesis that the cells had transdifferentiated. Instead, clusters of labeled cells were found along the rim of the enlarging canal, leading to the suggestion that cells were recruited into the epithelial tube. However, since the label was not specific to the cells of the fusion plate, its subsequent localization does not unequivocally allow for fate mapping. Even if such cells had originated at the fusion plate, it is still possible that they were destined to die, since apoptotic cells were observed in similar locations in normal chicken ears in the present study.

It is still formally possible that the process of semicircular canal formation may vary between species, although this would be surprising for such a complex and fundamental aspect of ear morphogenesis. Nonetheless, there is precedent for interspecific differences in otic vesicle development: the hollow center

of the otic vesicle of the zebrafish forms by cavitation of a solid ball of cells (Haddon and Lewis, 1996) whereas in birds and mammals it arises by invagination and pinching off of an epithelial sheet and is therefore 'hollow' from the start. An analogous process occurs during neural tube formation, with fish differing from amniotes in that cavitation rather than invagination is used to hollow out the center of a solid cord of neural cells (Schmitz et al., 1993).

Finally, we cannot infer that death is the only possible fate for the cells of the fusion plates. It is conceivable that cell death occurs in concert with other mechanisms, such as epithelial-to-mesenchymal transformation and/or the recruitment of cells into the expanding canal. Epithelial-to-mesenchymal transformation seems the least likely mechanism in the chicken, in view of the fact that the basal lamina appears to remain intact throughout the morphogenesis of the canal. Fate mapping experiments are necessary to ascertain the relative roles of each of the various processes in the dispersal of fusion plate cells in the chicken embryo. The interpretation of such experiments will depend upon whether the dying cells (along with their fate marker) are ultimately lysed in other cells (such as macrophages, neighboring epithelial cells, or surrounding mesenchymal cells) or whether they undergo autolysis (Clarke, 1990). It is clear from the present study that degenerating nuclear material ends up, at least transiently, in the expanding canals and in the mesenchyme. This distribution of apoptotic bodies may confound fate mapping experiments with short survival times.

Sculpting complex structures using focal programmed cell death

In the context of normal development, programmed cell death is a widely used mechanism for generating the normal number of cells, for eliminating transient embryological structures (such as the anuran tail) and for the separation of parts of the embryo from one another (Glucksmann, 1951). However, there are relatively few examples of the application of programmed cell death in the patterning of complex tissues. One renowned example is digit formation in the developing limb bud of vertebrates, during which the mesenchymal tissue in the interdigital region 'disappears' by programmed cell death (Hammar and Mottet, 1971). This process converts the flattened limb palette into the digit-dominated structure so characteristic of the vertebrate hand or foot. The absence of interdigital cell death, such as in *Fused toes* mutant mice, results in syndactyly, or failure of the digits to separate (van der Hoeven et al., 1994). In the embryonic chicken, manipulations that reduce or enhance interdigital cell death give rise to abnormal feet (Zou and Niswander, 1996; Ganan et al., 1996; Yokouchi et al., 1996). We propose that the focal cell death in the center of each semicircular canal during ear development is analogous to the focal cell death in the interdigital regions during limb development in that both play a role in patterning. It should be noted, however, that these two processes involve two distinct tissue types (mesenchymal versus epithelial). We conclude that controlling the spatial and temporal aspects of programmed cell death can be a general process leading to pattern formation in complex structures, regardless of the histotypical tissue type.

Epithelial-epithelial fusions during embryogenesis

There are several other morphogenetic processes that involve the approach, fusion and clearing of two apposing epithelial sheets in vertebrate embryos. Some notable examples are the fusion of the palate at the midline, the formation of the septa of the heart, and the separation from the ectoderm of the neural tube, the lens and the otic vesicle. In each case, a similar topological problem presents itself: two epithelial sheets come into contact at their apical surfaces and appear to fuse. Such a process should not be conducive to forming cell-cell contacts, because of the barrier function of the apical surface of epithelia. The 'problem' appears to be overcome by several different mechanisms at the cellular level.

Consider first the case of palate formation of the mammalian embryo. Historically, disappearance of fusion plates (called the midline seams) was cited as a classic example of programmed cell death required for epithelial fusion (reviewed by Ferguson, 1988). In fact, cell death may be required to remove the apical-most layer of this epithelium, allowing the underlying basal cells to come into contact and fuse. In contrast, a role of cell death in clearing the midline seam after fusion is no longer favored. Instead, two groups have data supporting epithelial-to-mesenchymal transformation (Fichett and Hay, 1989; Schuler et al., 1992; Griffith and Hay, 1992), while data from another group supports a third alternative, that the cells ultimately become part of the remaining epithelial sheets (Carrette and Ferguson, 1992). However, it should be noted that cell death in this system has not been examined with the TUNEL protocol, nor has it been experimentally blocked to assess its function.

Consider next those examples in which an ectodermal structure invaginates and then delaminates from the overlying ectoderm. For the neural tube, it is well established that the migratory neural crest cells arise at the junction between the overlying ectoderm and the delaminating neural tube. Here the topological problem of apposing epithelial sheets could be solved by continued delamination of the cells at the interface, that is by epithelial-to-mesenchymal transformation (Duband et al., 1995), although a specific role for programmed cell death has yet to be investigated. In contrast, during formation of both the lens vesicle and the otic vesicle, there is evidence that cell death is present near the sites of separation from the overlying ectoderm (Glucksmann, 1951; Represa et al., 1990; Marovitz et al., 1977). Whether cell death is crucial for the process of vesicle delamination in either of these structures requires further study.

What is the purpose of cell death at the fusion plates?

We are still left to ponder what the precise role of cell death in the fusion plate may be. Is cell death required to disrupt the integrity of the epithelial layer, thereby allowing for apposing cells to intermingle? Is cell death needed to break cell-cell contacts among adjacent cells, thereby permitting individual cells to lose their apical-basal polarity and establish a topographically reversed relationship with the cells of the apposing sheet? Or is cell death simply required for the disposal and clearing of the unwanted cells once fusion has taken place? Our data cannot clearly distinguish from among these possibilities, which are themselves not mutually exclusive. It seems likely that cell death is required at the initial stages of epithelial fusion since, in the most severely disrupted canals, cells from the two apposing sides were unable to intermingle and fuse in

the absence of cell death. Cell death also appears to be required later, to clear the fusion plate cells, since this process was delayed in many of the ears in which *bcl-2* was overexpressed.

We thank Amy Kiernan and Rick Libby for comments on the manuscript, Marielle Langlois for technical assistance, Stephen H. Hughes for RCASBP(B)/*bcl-2*, and Barbara Barres for stimulating our interest in cell death in the ear. This work was supported by the March of Dimes Birth Defects Foundation and by a Clare Boothe Luce Professorship (to D. M. F.).

REFERENCES

Alvarez, I. S. and Navascués, J. (1990). Shaping, invagination, and closure of the chick embryo otic vesicle: Scanning electron microscope and quantitative study. *Anat. Rec.* **228**, 315-326.

Bartolami, S., Goodyear, R., and Richardson, G. (1991). Appearance and distribution of the 275kD hair-cell antigen during development of the inner ear. *J. Comp. Neurol.* **314**, 777-788.

Bissonnette, J. P. and Fekete, D. M. (1996). Standard atlas of the gross anatomy of the developing inner ear of the chicken. *J. Comp. Neurol.* **368**, 620-630.

Carrette, M. J. M. and Ferguson, M. W. J. (1992). The fate of medial edge epithelial cells during palatal fusion in vitro: An analysis by DiI labeling and confocal microscopy. *Development* **114**, 379-388.

Clarke, P. G. H. (1990). Developmental cell death: morphological diversity and multiple mechanisms. *Anat. Embryol.* **181**, 195-213.

Davies, A. M. (1995). The Bcl-2 family of proteins, and the regulation of neuronal survival. *Trends in Neuroscience* **18**, 355-358.

Duband, J. L., Monier, F., Delannet, M. and Newgreen, D. (1995). Epithelium-mesenchyme transition during neural crest development. *Acta. Anat.* **154**, 63-78.

Fekete, D. M and Cepko, C. L. (1993). Replication-competent retroviral vectors encoding alkaline phosphatase reveal spatial restriction of viral gene expression/transduction in the chick embryo. *Mol. Cell. Biol.* **13**, 2604-2613.

Ferguson, M. W. J. (1988). Palate development. *Development* **103 (Supplement)**, 41-60.

Fichett, J. E. and Hay, E. D. (1989). Medial edge epithelium transforms to mesenchyme after embryonic palatal shelves fuse. *Dev. Biol.* **131**, 455-474.

Fritzsch, B., Barald, K. F. and Lomax, M. I. (1997). Early embryology of the vertebrate ear. In *Development of the Auditory System* (eds E. W. Rubel, A. N. Popper, R. R. Fay). Springer Handbook of Auditory Research. Vol. XII. New York: Springer (In Press).

Ganan, Y., Macias, D., Duterque-Coquillaud, M., Ros, M. A. and Hurle, J. M. (1996). Role of TGFs and BMPs as signals controlling the position of the digits and the areas of interdigital cell death in the developing chick limb autopod. *Development* **122**, 2349-2357.

Gavrieli, Y., Sherman, Y. and Ben-Sasson, A. (1992). Identification of programmed cell death in situ via specific labeling of nuclear DNA fragmentation. *J. Cell Biol.* **119**, 493-501.

Givol, I., Tsarfaty, I., Resau, J., Rulong, S., Pinto da Silva, P., Nasioulas, G., DuHadaway, J., Hughes, S. H. and Ewert, D. L. (1994). Bcl-2 expressed using a retroviral vector is localized primarily in the nuclear membrane and the endoplasmic reticulum of chicken embryo fibroblasts. *Cell Growth Differ.* **5**, 419-429.

Glucksmann, A. (1951). Cell deaths in normal vertebrate ontogeny. *Biological Review* **26**, 29-86.

Griffith, C. M. and Hay, E. D. (1992). Epithelial-mesenchymal transformation during palatal fusion: carboxyflourescein traces cells at light and electron microscopic levels. *Development* **116**, 1087-1099.

Haddon, C. H. and Lewis, J. H. (1991). Hyaluronan as a propellant for epithelial movement: the development of semicircular canals in the inner ear of Xenopus. *Development* **112**, 541-550.

Haddon, C. H. and Lewis, J. (1996). Early ear development in the embryo of the zebrafish, *Danio rerio*. *J. Comp. Neurol.* **365**, 113-128.

Hamburger, V. and Hamilton, H. L. (1951). A series of normal stages in the development of the chick embryo. *J. Morph.* **88**, 49-91.

Hammar, S. P. and Mottet, N. K. (1971). Tetrazolium salt and electron-microscopic studies of cellular degeneration and necrosis in the interdigital areas of the developing chick limb. *J. Cell Sci.* **8**, 229-251.

Hay, B. A., Wolff, T. and Rubin, G. M. (1994). Expression of baculovirus P35 prevents cell death in *Drosophila*. *Development* **120**, 2121-2129.

Homburger, S. A. and Fekete, D. M. (1996). High efficiency gene transfer into the embryonic chicken CNS using B-subgroup retroviruses. *Dev. Dynamics* **206**, 112-120.

Kiernan, A. E. and Fekete, D. M. (1997). In vivo gene transfer into the embryonic inner ear using retroviral vectors. *Audiology and Neuro-Otology* **2**, 12-24.

Knowlton, V. Y. (1967). Correlation of the development of membranous and bony labyrinths, acoustic ganglia, nerves, and brain centers in the chick embryo. *J. Morph.* **121**, 179-208.

Marovitz, W. F., Shugar, J. M. and Khan, K. M. (1976). The role of cellular degeneration in the normal development of (rat) otocyst. *Laryngoscope* **86**, 1413-1425.

Marovitz, W. F., Khan, K. M. and Schulte, T. (1977). Ultrastructural development of the early rat otocyst. *Annals of Otology, Rhinology and Laryngology* **86**, 9-28.

Martin, P. and Swanson, G. J. (1993). Descriptive and experimental analysis of the epithelial remodellings that control semicircular canal formation in the developing mouse inner ear. *Dev. Biol.* **159**, 1-10.

Morgan, B. A. and Fekete, D. M. (1996). Manipulating gene expression with replication competent retroviruses. In *Methods in Avian Embryology* (ed. M. Bronner-Fraser), pp. 185-218. San Diego: Academic Press.

Reed, J. C. (1994). Bcl-2 and the regulation of programmed cell death. *J. Cell Biol.* **124**, 1-6.

Represa, J. J., Moro, J. A., Pastor, F., Gato, A. and Barbosa, E. (1990). Patterns of epithelial cell death during early development of the human inner ear. *Annals of Otology, Rhinology and Laryngology* **99**, 482-488.

Riedl, A. E., Garcia, L. F., Cotanche, D. A. and Fekete, D. M. (1997). Programmed cell death is involved in chicken ear development. *Assoc. Res. Otolaryngol. Abs.* **Abstract 522**, 131.(Abstr.)

Schmitz, B., Papan, C. and Campos-Ortega, J. A. (1993). Neurulation in the anterior trunk region of the zebrafish *Brachydanio rerio*. *Roux's Arch. Dev. Biol.* **202**, 250-259.

Schuler, C. F., Halpern, D. E., Guo, Y. and Sank, A. C. (1992). Medial edge epithelium fate traced by cell lineage analysis during epithelial-mesenchymal transformation in vivo. *Dev. Biol.* **154**, 318-330.

van der Hoeven, F., Schimmang, T., Volkmann, A., Mattei, M.-G., Kyewski, B. and Ruther, U. (1994). Programmed cell death is affected in the novel mouse mutant *Fused toes (Ft)*. *Development* **120**, 2601-2607.

Waterman, R. E. and Bell, D. H. (1984). Epithelial fusion during early semicircular canal formation in the embryonic zebrafish, *Brachydanio rerio*. *Anat. Rec.* **210**, 101-114.

Yokouchi, Y., Sakiyama, J-i., Kameda, T., Iba, H., Suzuki, A., Ueno, N. and Kuroiwa, A. (1996). BMP-2/-4 mediate programmed cell death in chicken limb buds. *Development* **122**, 3725-3734.

Zou, H. and Niswander, L. (1996). Requirement for BMP signaling in interdigital apoptosis and scale formation. *Science* **272**, 738-741.

(Accepted 11 April 1997)